POSACC: Position-Accuracy Based Adaptive Beaconing Algorithm for Cooperative Vehicular Safety Systems

SANDY BOLUFÉ[1], CESAR A. AZURDIA-MEZA [1], (Member, IEEE),
SANDRA CÉSPEDES [1], (Senior Member, IEEE),
SAMUEL MONTEJO-SÁNCHEZ [2], (Member, IEEE),
RICHARD DEMO SOUZA [3], (Senior Member, IEEE),
AND EVELIO M. G. FERNANDEZ [4], (Member, IEEE)

[1]Department of Electrical Engineering, Universidad de Chile, Santiago 8370451, Chile
[2]Programa Institucional de Fomento a la I+D+i, Universidad Tecnológica Metropolitana, Santiago 8940577, Chile
[3]Department of Electrical and Electronics Engineering, Federal University of Santa Catarina, Florianópolis 88040-900, Brazil
[4]Department of Electrical Engineering, Federal University of Paraná, Curitiba 81531-990, Brazil

Corresponding author: Cesar A. Azurdia-Meza (cazurdia@ing.uchile.cl)

ABSTRACT Cooperative vehicular safety systems are expected to revolutionize the driving experience by providing road safety applications based on incident detection. Two vital quality parameters for cooperative safety applications are the position accuracy and communication reliability of the status information. The receiver may take erroneous decisions if the received data does not correspond to the latest situation of the transmitter (e.g., position, velocity, and trajectory of the target vehicle). In this paper, we propose and evaluate a POSition-ACCuracy (POSACC) based adaptive beaconing algorithm for cooperative vehicular safety systems. POSACC integrates three different control mechanisms to guarantee specific performance metrics. It adopts the position accuracy and communication reliability as the highest priority metrics, due to their direct impact on the vehicle's systems capability to avoid potential traffic accidents in real-time. In addition, it guarantees the priority metrics, maintaining the vehicle's warning distance, channel load, and end-to-end latency into the operative range of cooperative safety applications. POSACC is compared with three different state-of-the-art adaptive beaconing algorithms; ETSI DMG, LIMERIC, and DC-BTR&P. Extensive evaluation results show that POSACC successfully controls the beacon rate, transmission power, and the size of the minimum contention window. Simulation results also demonstrate that POSACC is more effective than the benchmark algorithms by guaranteeing the operational requirements of cooperative safety applications in a wider range of traffic situations.

INDEX TERMS Adaptive beaconing algorithm, communication reliability, cooperative safety applications, cooperative vehicular safety systems, position accuracy.

I. INTRODUCTION

Cooperative vehicular safety systems are being designed to provide accident-free and efficient road systems [1]. The new paradigm relies on equipping the vehicle with wireless communication devices to increase its perception about the

The associate editor coordinating the review of this manuscript and approving it for publication was Muhammad Naeem .

surrounding environment. Cooperative safety applications aim to detect potential crashes on the road and to notify vehicles in advance. The communication on these systems relies on the IEEE 802.11p [2] radio access technology in the 5.9 GHz frequency band, which specifies the medium-access-control (MAC) and physical (PHY) layers of Wireless Access in Vehicular Environments (WAVE) [3]. The IEEE 802.11p MAC layer is based on the Carrier Sense Multiple

Access with Collision Avoidance (CSMA/CA) protocol and includes the Outside of the Context of a Basic Service Set (OCB) operation mode recently defined in [4]. The IEEE 802.11p PHY layer is based on the IEEE 802.11a standard, but it uses channels of 10 MHz to reduce the negative impact of multipath delay spread and Doppler effect [5].

Cooperative vehicular safety systems rely on the continuous exchange of status information between neighboring vehicles on a common control channel (CCH). To make neighbors aware of its presence, each vehicle regularly transmits one-hop broadcast messages, called *beacons*. The beacons are formally known as Basic Safety Messages (BSM) [6] in the US or Cooperative Awareness Messages (CAM) [7] in Europe. These messages include information about the status of the transmitting vehicle; such as its position, speed, acceleration, and heading. The beaconing process allows the receiving vehicle to create a Local Dynamic Map (LDM) based on the status information of its neighborhood [7]. The status information is used by cooperative safety applications to detect and mitigate potential crashes in real-time (e.g., the crash risk can be estimated by analyzing the movement status of vehicles) [7].

Finding the appropriate beacon transmission rate for each vehicular scenario is essential for the proper performance of cooperative safety applications. The beacon transmission rate is directly related to the position accuracy perceived by neighboring vehicles [8]. In realistic scenarios, some vehicles could have high dynamics (high speed and acceleration), whereas other vehicles could have low dynamics (low speed and acceleration). This may lead to differences in position accuracy since position error depends on beacon rate and vehicle dynamics. In traffic jams, a beacon transmission rate of 1 beacon/s could be enough to provide the position accuracy needed for most safety-related applications. However, this beacon rate is not enough to achieve the required level of position accuracy on a multi-lane high-speed highway with frequent lane changes. The technical report of the Vehicle Safety Communications Consortium (VSCC) [9] specifies that 10 beacon/s is the minimum beacon rate required to meet the position accuracy of several safety-related applications, while some safety-critical applications can demand a beacon rate up to 50 beacon/s.

The operational requirements of cooperative safety applications can be defined mainly in terms of position accuracy, communication reliability, and end-to-end latency [10], [11]. The European Telecommunication Standards Institute (ETSI) has specified in the technical specification ETSI TS 101 539-3 [10] that cooperative safety-critical applications, such as Longitudinal Collision Risk Warning (LCRW) (e.g., safety-relevant lane change and safety-relevant vehicle overtaking), demand a position accuracy equal or less than 1 m with a confidence level of 95 %, a communication range of 300 m in a line of sight situation and when the channel load is at a relaxed state, and an end-to-end latency equal or less than 300 ms. Similarly, cooperative safety-critical applications, such as Intersection Collision Risk Warning (ICRW)

(e.g., turning collision risk warning and merging collision risk warning) defined by ETSI in ETSI TS 101 539-2 [11], require a position accuracy equal or better than 2 m with a confidence level of 95 %, a communication range of 300 m in a line of sight situation and when the channel load is at a relaxed state, and an end-to-end latency equal or less than 300 ms. ETSI also specifies in [10], [11] that the required communication range may be reduced in certain situations (e.g., in congested channel situations).

Congestion and awareness control approaches have been proposed in the literature [12], [13] to provide reliable and efficient vehicular communications. However, both approaches have drawbacks in terms of road safety. Congestion control approaches [14]–[17] aim at keeping the channel load below a certain target threshold and to achieve local/global fairness. However, these approaches usually do not consider the operational requirements of safety-related applications or vehicle dynamics. In contrast, awareness control approaches [7], [18]–[21] can consider road safety or vehicle dynamics, but they usually are not designed to simultaneously satisfy the operational requirements of cooperative safety applications. Furthermore, channel busy ratio (CBR) is generally used as a priority metric; however other critical metrics directly related to road safety, such as position error, packet collision rate, packet delivery ratio (PDR), and end-to-end latency are not considered.

A. CHALLENGES OF BEACONING APPROACHES
A high beacon rate is desirable from the viewpoint of providing fresh information and ensuring that vehicles have high levels of awareness [20]. However, a high beacon rate also could lead to a congested channel, especially, in scenarios with a high vehicular density. Channel congestion leads to a degradation of communication reliability caused by packet collisions [22]. Even if the channel is not congested, a high beacon transmission rate can still cause severe interference due to the hidden terminal problem and the CSMA/CA Distributed Coordination Function (DCF) procedure of IEEE 802.11p [23]. Simultaneously, packet collisions have a negative impact on position accuracy. This underlying trade-off also applies to the beacon transmission power [24]. A high beacon transmission power increases the probability of successful reception of a single transmission, but at the same time increases the probability of packet collisions for all transmissions.

A contradictory behavior is also observed regarding the size of the minimum contention window used by the backoff algorithm in IEEE 802.11p. Beacons are usually transmitted with the highest priority access category [13]. Due to the short temporal validity of beacons, the size of the minimum contention window used by the backoff algorithm in IEEE 802.11p is often kept small. However, reducing the size of the minimum contention window increases the probability of packet collisions in broadcast communications where no exponential backoff is considered [25]. The probability of packet collisions can be reduced by increasing the size of the

minimum contention window; but, it has a negative effect on end-to-end latency.

Meeting the operational requirements of cooperative safety applications is a very challenging task. The responsibility for meeting the requirements of a specific performance metric in the worst-case scenario (more demanding applications) can lead to not meeting the requirements of these and other applications in other metrics. In this context, we propose a novel POSition-ACCuracy (POSACC) based adaptive beaconing algorithm for cooperative vehicular safety systems. It aims to satisfy the operational requirements of cooperative safety applications. POSACC is compared with relevant state-of-the-art beaconing algorithms via a realistic simulation framework and considering performance metrics directly related to road safety.

The contribution of this paper is threefold:

1) We adopt the position accuracy and communication reliability as the highest priority metrics due to their direct impact on the decision-making process, in real-time, of cooperative safety applications. We establish a design strategy that reduces the conflict between the required goals. The strategy focuses on providing the position accuracy and communication reliability required by cooperative safety applications, maintaining the vehicle's warning distance, channel load, and end-to-end latency into the operative range of the cooperative safety applications.

2) We design three different control mechanisms to guarantee specific performance metrics. We design a beacon rate control mechanism that adapts the beacon rate depending on vehicle movement status to achieve the desired position accuracy. In addition, we design a transmission power control mechanism that computes the vehicle's transmission power depending on its movement status to maximize the probability of successful reception of beacon messages at the target warning distance. Finally, we design a control mechanism that computes the size of the minimum contention window depending on the maximum reported size of the LDM database in order to minimize the probability of packet collisions.

3) We propose an adaptive beaconing algorithm, called POSACC, to simultaneously guarantee the operational requirements of cooperative safety applications. Extensive evaluation results show that POSACC successfully controls the beacon rate, transmission power, and the size of the minimum contention window. Simulation results also demonstrate that POSACC is more effective than three state-of-the art algorithms: ETSI DMG [7], LIMERIC [15], and DC-BTR&P [26], by adapting to the vehicle dynamics as well as guaranteeing the operational requirements of cooperative safety applications in a wider range of traffic situations.

The remainder of this paper is organized as follows. Section II reviews related work. Section III introduces the control mechanisms and POSACC algorithm. Section IV describes the simulation setup. Section V evaluates the performance of the proposed algorithm, whereas Section VI presents conclusions and future works.

II. RELATED WORK

In the ETSI EN 302 663 standard [27], ETSI has defined a 10 MHz common control channel for vehicular communications at 5.9 GHz, known as the ITS-G5 radio channel. To enable cooperative awareness within ITS-G5, ETSI also has delivered the standard ETSI EN 302 637-2 [7] specifying the rules for the exchange of CAMs. The cooperative awareness basic service is mandatory for all nodes operating in ITS-G5. In this service, vehicles regularly broadcast their status data by using the CSMA/CA protocol with no acknowledgments or retransmissions. One key problem of the beaconing activity is the channel congestion that can arise due to the aggregated load. In this context, ETSI has defined the Cross-Layer Decentralized Congestion Control (DCC) Management Entity to avoid overloading the ITS-G5 radio channel [28]. Channel congestion can limit the transmission of event-driven messages, such as the Decentralized Environmental Notification Messages (DENMs) defined by ETSI in ETSI EN 302 637-3 [29]. Channel congestion can also negatively affect the proper performance of cooperative safety applications. In the following, we overview some congestion and awareness control approaches.

Some examples of congestion control approaches available in the literature are PULSAR [14], LIMERIC [15], FABRIC [16], and DCC [17]. Two of the most important current congestion control approaches are PULSAR [14] and LIMERIC [15]. Both approaches adapt the beacon rate based on the channel load and set the transmission power to a fixed value. PULSAR relies on a binary rate control using the Additive Increase Multiplicative Decrease (AIMD) technique. To fulfill the global fairness design principle, vehicles share two-hop CBR information. In LIMERIC, the underlying function linearly controls the beacon rate of each vehicle according to local CBR measurements. LIMERIC converges to a fair and efficient channel utilization in deterministic environments. To ensure the convergence in very dense scenarios, it uses an effective gain saturation technique. PULSAR and LIMERIC are able to maintain the channel load below a certain target threshold independently of the vehicular traffic density. In LIMERIC, noisy CBR measurements produce unfairness in rate allocations [30].

FABRIC [16] is based on a network utility maximization problem. In FABRIC, the beacon rate of each vehicle in the one-hop neighborhood is recursively optimized. To enable this, it is proposed that all vehicles share their beacon rates. The main drawback of FABRIC is controlling the speed of convergence in practical scenarios [20]. ETSI has also specified a set of DCC mechanisms [17] that adapt the beacon transmission parameters to keep the channel load below a target threshold. All the mechanisms rely on a state machine that distinguishes three states: *relaxed*, *active*,

and *restrictive*, in increasing order of channel congestion. State transitions are driven by the channel load conditions locally measured by each node during a sampling interval. DCC is naturally oscillatory, which implies unstable state transitions [31].

Several awareness control approaches exist in the literature. For example, the awareness control approach proposed by ETSI is the dynamic message generation mechanism [7], which we call here ETSI DMG. It adapts the beacon rate depending on the changes in position, velocity, and heading of the transmitting vehicle. This approach aims to limit the position error perceived by neighboring vehicles while implicitly controls the channel load. ETSI DMG has a synchronization problem for cooperative maneuvers that degrades its performance [32]. It also suffers from a divergence effect that leads to oscillations in the beacon rate [33]. IVTRC [18] is an awareness control approach that also considers the position accuracy as a design goal. It controls the beacon rate depending on differences from position predictions. However, beaconing based on position prediction has serious drawbacks for road safety, as specified in [34]. Further, in situations where the channel load increases, IVTRC reduces the beacon transmission rate of vehicles at the cost of decreasing the position accuracy.

Other awareness control approaches available in the literature are INTERN [19], NORAC [20], TTCC [21], and DC-BTR&P [26]. INTERN [19] assigns the beacon transmission rates required by the applications, and then equitably shares the excess capacity. It also controls the transmission power to generate certain level of awareness. NORAC [20] is a rate and awareness distributed control approach based on non-cooperative game theory. The underlying congestion control mechanism limits the bandwidth usage of each vehicle and reduces the beaconing rate in congested situations. NORAC assigns a beacon transmission rate to each vehicle proportional to its requirements while ensuring fairness between vehicles with the same requirement. Similarly, TTCC [21] aims to satisfy the constraints on channel availability, whereas the safety of the surrounding traffic situation is captured with a time-to-collision metric. TTCC increases the beacon transmission rate of the vehicles involved in more dangerous situations, so it yields higher rates and better usage of channel capacity.

DC-BTR&P [26] is an awareness control approach designed to satisfy the position accuracy requirements of cooperative safety applications. This approach is based on the dynamic control of the beacon rate and transmission power. The underlying control mechanisms limit the position error perceived by neighboring vehicles and reduce packet collisions. However, such benefits are achieved at the cost of decreasing the communication range of vehicles with higher dynamics. This issue is critical for road safety because drivers need to be notified at a sufficient distance from the expected impact to initiate a maneuver, as defined by ETSI technical specifications [10], [11].

TABLE 1. Operational requirements of LCRW and ICRW applications.

Application	Position accuracy	Communication range†	End-to-end latency
LCRW [10]	≤ 1 m, 95 %	300 m	≤ 300 ms
ICRW [11]	≤ 2 m, 95 %	300 m	≤ 300 ms

† As specified by ETSI, the communication range may be reduced (e.g., in congested channel situations) but without affecting the safety time required by cooperative safety applications [10], [11].

A. LIMITATIONS RELATED TO ROAD SAFETY

The primary motive for using vehicular communications is to improve road safety. Therefore, congestion and awareness control approaches not only should prevent channel congestion or improve cooperative awareness, but also ensure the quality of service required for the proper performance of cooperative safety applications. ETSI specifies that safety applications such as LCRW [10] and ICRW [11] have strict operational requirements in terms of position accuracy, communication reliability, and end-to-end latency, as shown in Table 1. However, most of the current congestion and awareness control approaches have not been designed to satisfy the requirements simultaneously.

The main drawback of congestion control approaches such as PULSAR [14], LIMERIC [15], FABRIC [16], and DCC [17] is that they do not explicitly consider the operational requirements of cooperative safety applications or vehicle dynamics. Congestion control approaches generally adapt beacon rate based only on the channel load, without considering the traffic situation of neighboring vehicles. This could be critical for road safety in vehicular scenarios such as a highway with a traffic jam in one direction, resulting in a congested channel, and a free-flow condition in the opposite direction with high-speed vehicles. The vehicles in free-flow are forced to reduce their beacon rates due to channel congestion even if they require a high beacon rate to maintain a certain level of position accuracy. In addition, the interference generated by the vehicles in the traffic jam can significantly affect the communication reliability of vehicles in free-flow, reducing the effectiveness of cooperative safety applications.

Regarding current awareness control approaches, most of them have not been designed to simultaneously satisfy the operational requirements of cooperative safety applications. Some awareness control approaches aim to maintain a certain level of position accuracy. For instance, ETSI DMG [7] and IVTRC [18] adapt the beacon transmission rate according to the vehicle dynamics to limit the position error perceived by neighboring vehicles. ETSI DMG does not consider an additional control mechanism to guarantee communication reliability in dense traffic situations. IVTRC mitigates packet collisions, but at the cost of reducing the beacon rate, which directly affects the position accuracy. In contrast, INTERN [19] does not consider the position accuracy or vehicle dynamics. Furthermore, it also has difficulties to guarantee the beacon rates and warning distances required by the safety applications. This issue is represented by feasible regions [19] where the requirements of all vehicles could be satisfied without overloading the channel. Another drawback is that

the feasible regions change with the vehicular density, so it is a challenge to avoid the regions where the requirements are not satisfied.

NORAC [20] and TTCC [21] aim to improve cooperative awareness by increasing the beacon rate of certain vehicles. However, these approaches have not been designed to satisfy a pre-defined position accuracy, nor do they have a mechanism to mitigate packet collisions. Improving cooperative awareness is not sufficient to guarantee the quality of service required by safety-critical applications. The main reason is that increasing the beacon rate also leads to more packet collisions, especially for high vehicular densities and low minimum contention windows [25], [35]. Further, CBR is generally used as a priority metric, and other critical performance metrics directly related to road safety, such as position error, packet collision rate, PDR, and end-to-end latency are not considered.

Finally, DC-BTR&P [26] defines a minimum fixed transmission power independently of the vehicle dynamics. Further, it reduces packet collisions by decreasing the communication range of vehicles with higher dynamics. This issue is critical for road safety because vehicles with high speed should use a higher transmission power in order to increase their notification capacity. Another limitation is that vehicles adapt the beacon transmission parameters based on their own dynamics, without considering information from the surrounding environment. Therefore, in this paper, we design the POSACC approach to overcome these issues and guarantee the operational requirements of cooperative safety applications.

B. APPROACHES USED AS BENCHMARK

As a benchmark for comparison, we utilize three different beaconing approaches; ETSI DMG [7], LIMERIC [15], and DC-BTR&P [26]. ETSI DMG is the awareness control approach specified by European standards, whereas LIMERIC is one of the most important congestion control approaches available in the literature. ETSI DMG adapts the beacon rate depending on vehicle dynamics to provide a target position accuracy. In contrast, LIMERIC adapts the beacon rate based on the locally measured CBR to maintain the channel load below a certain target threshold and to achieve fairness. We also include our previous approach DC-BTR&P, which is an awareness control algorithm that adapts the beacon rate and transmission power to provide a target position accuracy and reduce interference. The evaluation of these beaconing approaches will help understand their benefits and limitations when referring to road safety.

III. PROPOSED ALGORITHM

This section presents the design of the POSition-ACCuracy (POSACC) based adaptive beaconing algorithm for cooperative vehicular safety systems. POSACC aims to satisfy the operational requirements of cooperative safety applications. The POSACC system architecture is illustrated in Fig. 1. We assume that each vehicle obtains its own location from
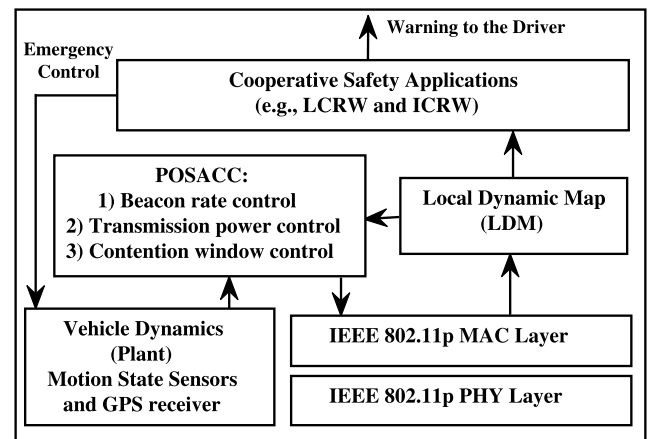

FIGURE 1. POSACC system architecture.

the Global Positioning System (GPS) device, as well as its own movement parameters (e.g., velocity, acceleration, and heading) from on-board sensors. Each vehicle also has an LDM database, where the beaconing information from its neighbors is stored. One entry is created for each neighboring vehicle. The LDM database provides information from the surrounding traffic situation (e.g., the number of neighboring vehicles as well as their movement parameters). Entries are updated at beacon receptions. If a neighbor does not announce its presence once the entry expiration time has been reached, the entry is erased from the LDM database. Cooperative safety applications require fresh status information to successfully detect possible threats. If a hazardous situation is detected, the safety-critical application provides warnings to the driver or it may trigger collision avoidance actions (e.g., in autonomous driving).

To fulfill the design goals, POSACC utilizes three different control mechanisms:

- **Beacon rate control**: it adapts the beacon rate depending on vehicle dynamics to provide the required position accuracy.
- **Transmission power control**: it adapts the transmission power depending on vehicle dynamics to guarantee the required warning distance.
- **Contention window control**: it takes advantage of the LDM database information to adapt the size of the minimum contention window by minimizing the probability of packet collisions.

In the following subsections, the control mechanisms and POSACC algorithm are presented in detail.

A. BEACON RATE CONTROL MECHANISM

The beacon rate control mechanism adapts the beacon rate in real-time to limit the position error perceived by neighboring vehicles. In this mechanism, the beacon rate is controlled according to the transmitter vehicle dynamics. Therefore, the beacon rate is reduced when the vehicle has low dynamics, alleviating the channel load and decreasing the interference
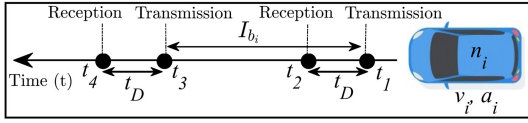
FIGURE 2. Relevant time parameters that determine the position accuracy.

on its neighbors. Furthermore, the resulting beaconing load is implicitly controlled by the relationship between average velocity and traffic density [34]. As a consequence, the channel load remains stable when more vehicles drive at lower velocities.

Fig. 2 illustrates relevant time parameters that influence position accuracy. If the event of looking up the vehicle's position in the LDM database is uniformly distributed between the minimum and maximum time difference of the beacon transmission event, the average position error ($\overline{E}$) perceived by neighboring vehicles is [34],

$$\overline{E} = \frac{E_{\min} + E_{\max}}{2}, \qquad (1)$$

where $E_{\min}$ is the minimum error resulting from the transmission delay (t_D), and $E_{\max}$ is the maximum error resulting from the beacon interval and transmission delay.

We assume constant acceleration during the beacon interval. So, from kinematic equations, $\overline{E}$ is expressed as a function of velocity (v_i) and acceleration (a_i) of the transmitting vehicle (n_i),

$$2\overline{E_i} = v_i t_D + I_{b_i}\left(v_i + \frac{a_i I_{b_i}}{2}\right) + t_D(a_i I_{b_i} + v_i), \qquad (2)$$

where I_{b_i} is the beacon interval of n_i (equal to the inverse of beacon transmission rate, R_{b_i}). We assume beacon messages of the same size (b_z) and equal data-rate (R_D), so t_D is the same for all vehicles, $t_D = b_z/R_D$.

A quadratic function, $f(I_{b_i}) = AI_{b_i}^2 + BI_{b_i} + C$, can be obtained from (2) as follows,

$$f(I_{b_i}) = a_i I_{b_i}^2 + 2(v_i + a_i t_D)I_{b_i} + 4(v_i t_D - \overline{E_i}). \qquad (3)$$

In the general case of $a_i \neq 0$, the discriminant (D) and solutions ($I_{b_{i\{1,2\}}}$) of the quadratic function are computed as follows,

$$D = 4\left[(v_i + a_i t_D)^2 - 4a_i\left(v_i t_D - \overline{E_i}\right)\right], \qquad (4)$$

$$I_{b_{i\{1,2\}}} = \frac{-v_i - a_i t_D \pm \left[v_i^2 + (a_i t_D)^2 - 2a_i\left(v_i t_D - 2\overline{E_i}\right)\right]^{\frac{1}{2}}}{a_i}. \qquad (5)$$

Otherwise, if $a_i = 0$, the solution (I_{b_i}) is computed using the linear equation,

$$I_{b_i} = \frac{2(\overline{E_i} - v_i t_D)}{v_i}. \qquad (6)$$

Fig. 3 shows the numerical solutions of the beacon interval by using (3) for different setups: acceleration (deceleration),
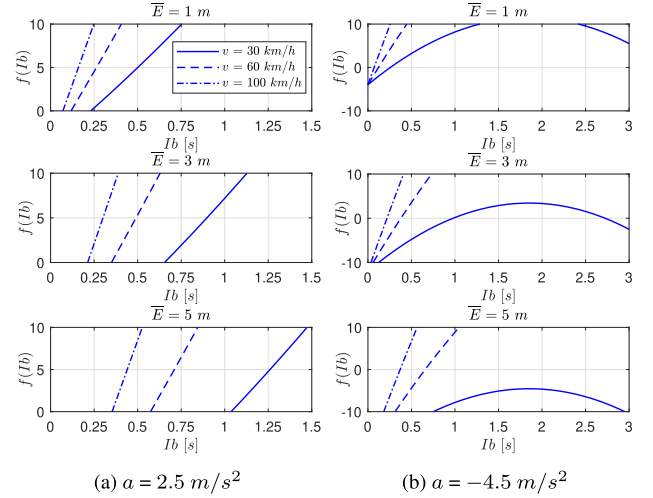

FIGURE 3. Numerical solutions of the beacon interval computed using (3) for $b_z = 378$ bytes and $R_D = 6$ Mbps [15], equivalent to a transmission delay of 500 μs.
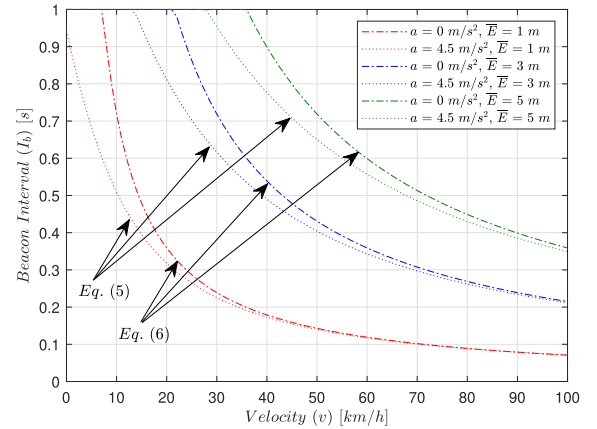

FIGURE 4. Beacon interval computed by using (5) and (6) for $b_z = 378$ bytes and $R_D = 6$ Mbps [15], equivalent to a transmission delay of 500 μs.

velocity, and average position error. To better relate the analysis with real traffic scenarios, velocity is shown in kilometers per hour. In the analysis only positive solutions ($0 < I_{b_i}$) are considered. A real root in the interval (0, 1] exists in most traffic situations. However, the root may be outside the range (0, 1] in acceleration (see Fig. 3a, $v_i = 30$ km/h and $\overline{E_i} = 5$ m), or even the root may not exist in deceleration (see Fig. 3b, $v_i = 30$ km/h and $\overline{E_i} = 5$ m). Fig. 4 shows the beacon interval computed by using (5) and (6) in the accelerated and uniform movement for different average position errors. As expected, an increase in velocity demands a shorter beacon interval to guarantee the desired position accuracy. The beacon interval not only responds to changes in velocity, but also to variations of acceleration. Note that the impact of acceleration is especially significant at low velocities since for a short beacon interval the velocity variation is low.

Algorithm 1 shows the steps followed by the beacon rate control mechanism to compute the beacon transmission rate in real-time depending on the vehicle movement status. On each beacon transmission, the vehicle n_i gets its velocity

---

Algorithm 1 Beacon Rate Control Mechanism

Data: $\{v_i, a_i, t_D, I_{b_c}, \overline{E_i}\}$
Result: $\{R_{b_i}\}$
begin

1 **if** *($v_i == 0$ && $a_i == 0$)* **then**
2 | $I_{b_i} \leftarrow 1$;
3 **else if** *($v_i >= 0$ && $a_i > 0$)* **then**
4 | *Compute* $I_{b_{i\{1,2\}}}$ using (5);
5 | $I_{b_i} \leftarrow maximum\{I_{b_{i\{1\}}}, I_{b_{i\{2\}}}\}$;
6 | **if** *($I_{b_i} > 1$)* **then**
7 | | $I_{b_i} \leftarrow 1$;
8 **else if** *($v_i > 0$ && $a_i == 0$)* **then**
9 | *Compute* I_{b_i} using (6);
10 | **if** *($I_{b_i} > 1$)* **then**
11 | | $I_{b_i} \leftarrow 1$;
12 **else if** *($v_i > 0$ && $a_i < 0$)* **then**
13 | *Compute D* using (4);
14 | **if** *(D > 0)* **then**
15 | | *Compute* $I_{b_{i\{1,2\}}}$ using (5);
16 | | $I_{b_i} \leftarrow maximum\{I_{b_{i\{1\}}}, I_{b_{i\{2\}}}\}$;
17 | | **if** *($I_{b_i} > I_{b_c}$)* **then**
18 | | | $I_{b_i} \leftarrow I_{b_c}$;
19 | **else if** *(D <= 0)* **then**
20 | | $I_{b_i} \leftarrow I_{b_c}$;
21 $R_{b_i} \leftarrow ceil(1/I_{b_i})$;
22 **return** R_{b_i};

---

v_i and acceleration a_i, and sets the desired position accuracy $\overline{E_i}$. Lines 1-20 involve the decisions associated depending on the movement status of n_i: repose (Line 1-2), the beacon transmission rate is set to 1 beacon/s equivalent to the minimum value required for the proper performance of the less demanding vehicular applications [7]; accelerated movement (Line 3-7), the beacon transmission rate is computed using (5); uniform movement (Line 8-11), the beacon transmission rate is computed according to (6); deceleration (Line 12-20), in order to notify with immediacy to surrounding vehicles a possible braking [34], it is set a critical beacon interval (I_{b_c}). We demonstrate the applicability of the beacon rate control mechanism in [26].

B. TRANSMISSION POWER CONTROL MECHANISM

We design the transmission power control mechanism based on the *"Dynamic Safety Shield"* concept presented by ETSI in [10], [11]. The dynamic safety shield is a virtual dynamic area surrounding the transmitting vehicle, as shown in Fig. 5. The size of the safety area is estimated by the transmitting vehicle in real-time. In order to react to a potential crash, a driver needs to be informed at a sufficient distance from the expected impact to initiate a maneuver [10], [11]. From
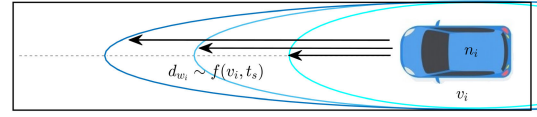

FIGURE 5. Dynamic safety shield for the transmitting vehicle n_i depending on its velocity v_i and the safety time t_s.

the transmitting vehicle's point of view, this means that it has to guarantee that its beacon messages are received within a certain distance, which we denote as target warning distance. The target warning distance (d_{w_i}) depends on the velocity v_i of the transmitting vehicle n_i, and the required safety time (t_s). Acceleration (deceleration) is not taken into account to avoid undesired oscillations on the warning distance. The safety time must consider the maximum latency time (e.g., 300 ms [10], [11]), the average driver's reaction time (e.g., 1.5 s [36]), the required action time (e.g., 0.75 s [37]), and a certain time margin.

We adopt the model based on Nakagami-m proposed by Killat et al. in [38] and used in [23], [26], [39] to compute the probability of successful reception of beacon messages in the presence of a single transmitter-receiver pair. This analytical model has been validated based on extensive evaluations via a discrete-event network simulator, achieving a perfect match [38]. The model combines the Nakagami-m distribution fast fading model and the Friis/Two-Ray-Ground path loss model. The probability of successful reception (P_{SR}) is computed depending on the distance (d) between the transmitter and receiver as follows [38],

$$P_{SR} = \begin{cases} e^{-3\left(\frac{d}{CR}\right)^2}\left(1 + 3\left(\frac{d}{CR}\right)^2 + \frac{9}{2}\left(\frac{d}{CR}\right)^4\right), \\ \qquad\qquad\qquad\qquad\qquad d \leq d_{c_o}, \quad (7) \\ e^{-3\gamma\left(\frac{d2}{CR}\right)^2}\left(1 + 3\gamma\left(\frac{d2}{CR}\right)^2 + \frac{9}{2}\gamma^2\left(\frac{d2}{CR}\right)^4\right), \\ \qquad\qquad\qquad\qquad\qquad d > d_{c_o}, \quad (8) \end{cases}$$

where the crossover distance, $d_{c_o} = 4\pi\left(\frac{h_t h_r}{\lambda}\right)$, depends on the wavelength of the signal (λ) and the height of the antennas (h_t), (h_r), and $\gamma = (d_{c_o})^{-2}$.

The Friis path loss model is considered for distances equal to or less than d_{c_o}. The Two-Ray-Ground path loss model is used for distances greater than d_{c_o}. The intended communication range (CR) depends on the configured transmission power. CR is the maximum achievable communication distance when only assuming path loss according to Friis/Two-Ray-Ground and neglecting fast fading effects. Fig. 6 shows P_{SR} for different intended communication ranges and distances between the transmitter and receiver over a crossover distance of 556 m, equivalent to a carrier frequency of 5.89 GHz and antenna heights of 1.5 m.

The transmission power control mechanism computes the optimal vehicle's transmission power (P_{T_i}) to maximize the probability of successful reception P_{SR} at the target warning distance. This control mechanism aims to ensure that the
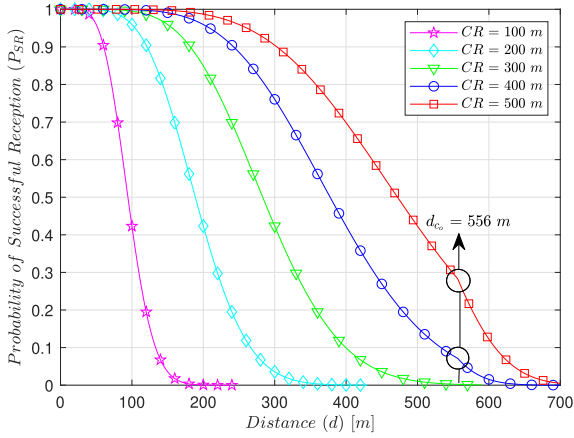
FIGURE 6. Probability of successful reception as a function of distance, using a carrier frequency of 5.89 GHz and antenna heights of 1.5 m.

beacons are received at the target warning distance with certain reliability (r_t). If the values of the intended communication range CR that satisfy the condition $P_{SR} \geq r_t$ are grouped into a discrete set $S = \{CR_1, CR_2, ..., CR_s\}$, the valid value of CR in (7) or (8) that maximizes P_{SR} at the target warning distance can be computed by solving the following optimization problem,

$$\max_{CR} \ P_{SR}$$
$$\text{s.t. } d = d_{w_i},$$
$$CR = CR_1 \in S \quad \forall \, P_{SR} \geq r_t. \tag{9}$$

Algorithm 2 describes the steps followed by the transmission power control mechanism to compute the optimal beacon transmission power in real-time depending on the vehicle movement status and the desired safety time. On each beacon transmission, the vehicle n_i gets its velocity v_i and sets the desired safety time t_s. The target warning distance d_{w_i} is computed according to basic kinematic equations (see Line 1). A minimum warning distance (d_{w_o}) is guaranteed in Lines 2-3. This is especially useful in low dynamic situations. The P_{SR} optimization function and the propagation model (used to compute the transmission power) are defined in Lines 4-9. We use the Newton-Raphson method to compute the intended communication range CR that maximizes P_{SR} at the target warning distance under the restriction $P_{SR} \geq r_t$ (see Line 10-14). Note that the first value of CR that satisfies the restriction is selected. Finally, the transmission power P_{T_i} is computed by evaluating the valid value CR_1 in the chosen model (see Line 15).

C. CONTENTION WINDOW CONTROL MECHANISM

IEEE 802.11p [2] considers the DCF procedure for medium contention. It includes the Hybrid Coordination Function (HCF), which provides prioritization techniques according to IEEE 802.11e. HCF defines different Arbitration Inter-Frame Space (AIFS) and contention window range depending on the access category (priority) of the packet. Highest priority packets have the shortest AIFS and the shortest contention

---

Algorithm 2 Transmission Power Control Mechanism

Data: $\{v_i, t_s, r_t, d_{w_o}, d_{c_o}\}$
Result: $\{P_{T_i}\}$
begin

1     $d_{w_i} \leftarrow v_i t_s$;
2   **if** $(d_{w_i} < d_{w_o})$ **then**
3        $\lfloor \ d_{w_i} \leftarrow d_{w_o}$;
4   **if** $(d_{w_i} <= d_{c_o})$ **then**
5        $P_{SR} \leftarrow$ (7) with $d \leftarrow d_{w_i}$;
6        $\lfloor P_T \leftarrow Friis\ model$ [25];
7   **else if** $(d_{w_i} > d_{c_o})$ **then**
8        $P_{SR} \leftarrow$ (8) with $d \leftarrow d_{w_i}$;
9        $\lfloor P_T \leftarrow Two\text{-}Ray\text{-}Ground\ model$ [25];
10    $CR_k \leftarrow d_{w_i}$;
11   **while** $P_{SR} < r_t$ **do**
12        $CR_{k+1} \leftarrow CR_k - P'_{SR}(CR_k)/P''_{SR}(CR_k)$;
13        $P_{SR} \leftarrow P_{SR}(CR_{k+1})$;
14        $CR_k \leftarrow CR_{k+1}$;
15    $P_{T_i} \leftarrow P_T(CR_{k+1})$;
16   **return** P_{T_i};

---

window to ensure a high probability of medium access. The initial contention window size is limited by the minimum contention window. For broadcast communication, there is no error-handling (e.g., no acknowledgments) and hence no exponential backoff growth [25]. As the contention window size is not increased, the size of the minimum contention window always defines the upper limit for the backoff counter. This limits the prioritization and increases the probability of packet collisions.

To compute the probability of packet collisions, we utilize the analytical model proposed by Bianchi in [40]. Bianchi's work is regarded as a standard in this research field. His model allows analyzing the performance of broadcast communications in vehicular networks based on IEEE 802.11p [25], [41], [42]. Applying Bianchi's model to vehicular communications where no exponential backoff is considered, the probability of packet collisions (p) can be computed as follows,

$$p = 1 - (1 - \tau)^{N-1}, \tag{10}$$

where N is the number of contending vehicles, and τ is the probability of a vehicle transmitting in a randomly chosen slot within the contention window size (CW) with no exponential backoff,

$$\tau = \frac{2}{CW + 1}. \tag{11}$$

Fig. 7 shows the probability of packet collisions for integer values[1] of CW in the range from 3 to 1023 [4]. Note that

---

[1] As specified in [4], CW is divided into equidistant time slots. The valid range of integers for CW is between 3 to 1023. The length of each time slot is 13 μs.
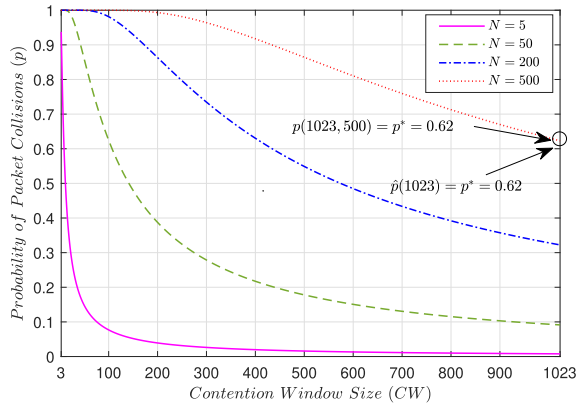
FIGURE 7. Probability of packet collisions according to the contention window size for different numbers of contending vehicles.

FIGURE 8. Numerical solutions of the minimum contention window computed by using (12) for $CW_{max} = 1023$ and $N_{max} = 500$.

the probability of packet collisions p is significantly high for small values of minimum contention windows, even if there is a low number of contending vehicles. Since interference cannot be completely eliminated in the IEEE 802.11p DCF procedure, the proposed control mechanism focuses on achieving the lowest possible value of the probability of packet collisions.

We design the contention window control mechanism to perform a linear distribution of the size of CW according to N. Let CW_{max} be the maximum value of CW and N_{max} be the maximum value of N. We denote as p^* the probability of packet collisions resulting from the evaluation of N_{max} and CW_{max} in (10) and (11), respectively. We utilize the linear function of the probability of packet collisions $\hat{p} = mCW$ that satisfies the condition $\hat{p}(CW_{max}) = p^*$, so the slope is $m = \frac{p^*}{CW_{max}}$. The solution $CW > 0$ for each $N > 1$ that satisfies the condition $p(CW, N) = \hat{p}(CW)$ (intersection point) can be computed by finding the zero of the following function,

$$P(CW) = 1 - \left(1 - \frac{2}{CW + 1}\right)^{N-1} - mCW. \quad (12)$$

The value of CW that minimizes P can be computed by solving the optimization problem,

$$\min_{CW} P$$

$$\text{s.t. } p^* = 1 - \left(1 - \frac{2}{CW_{max} + 1}\right)^{N_{max}-1},$$

$$m = \frac{p^*}{CW_{max}},$$

$$N > 1. \quad (13)$$

We design the control mechanism to provide the lowest value of p by using Bianchi's model when $CW = CW_{max}$ and $N = N_{max}$. For example, if $CW_{max} = 1023$ and $N_{max} = 500$, the lowest value of p according to Bianchi's model is $p(1023, 500) = p^* = 0.62$ (see Fig. 7). However, $\hat{p}(1023) = p^* = 0.62$ is the maximum value of probability of packet collisions according to $\hat{p}$. As we are interested in the intersection point between both functions, the optimal
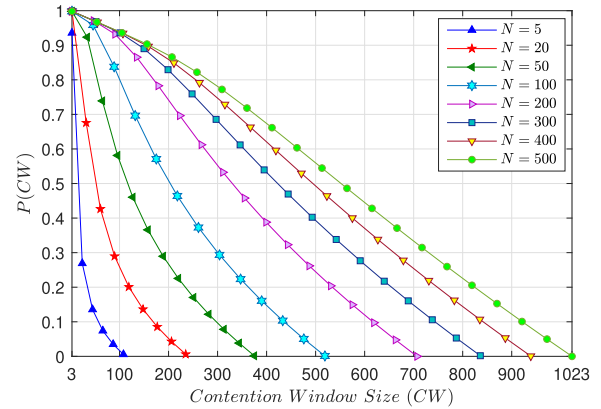
value of the minimum contention window CW provides the lower probability of packet collisions in the interval $(0, p^*]$, for each N in the interval $1 < N \leq N_{max}$ following a linear distribution. Fig. 8 shows the numerical solutions of CW computed by using (12) for different numbers of contending vehicles.

The proposed mechanism focuses on the collision domain of the transmitting vehicle in saturation condition, as specified by Bianchi's model assumptions [40]. The saturation condition assumption means that the control mechanism is able to operate in the worst-case scenario. This is a key design assumption since communication reliability is critical in safety communications. We reduce the number of contending vehicles N to the number of neighbors of the transmitting vehicle. This is a valid assumption since Bianchi's model [40] only focuses on the collision domain of the transmitter, neglecting the impact of the hidden terminals. Further, computing the number of contending vehicles in ad-hoc scenarios is a challenge because it involves the vehicles within the carrier-sensing-range.

To fulfill the steady-state principle of Bianchi's model [40], vehicles compute the optimal size of CW based on the maximum LDM database size ($\hat{N}$) reported on their neighborhood. Vehicles attach to the beacon the maximum value between its LDM database size and the maximum size announced by their neighbors, as shown in Fig. 9. Initially, vehicles n_1 and n_2 announce that their LDM databases are empty. At step 3, the vehicle n_3 announces a maximum LDM database size equal to 2. At step 5, the maximum size reported by the vehicles converges to the same value. The dissemination process allows vehicles to see the system in a steady-state.

Algorithm 3 describes the steps followed by the contention window control mechanism to compute the optimal size of the minimum contention window in real-time. On each beacon transmission, the vehicle n_i gets the maximum LDM database size $\hat{N}_i$ reported on its neighborhood. Lines 1-13 involve the decisions associated with the calculation of CW_i depending on $\hat{N}_i$. The smallest size of the minimum contention window CW_{min} is set in Lines 1-2. The Newton-Raphson method is
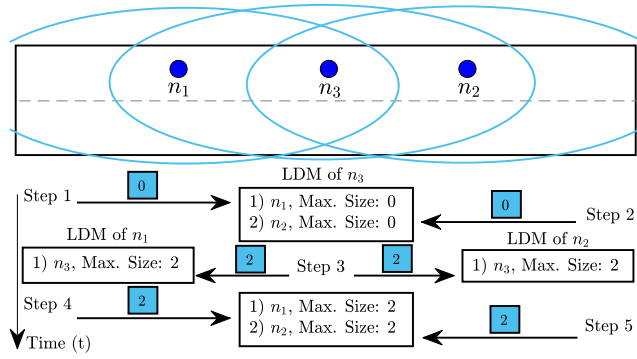
FIGURE 9. Representation of the LDM database size dissemination process.

Algorithm 3 Contention Window Control Mechanism

Data: $\{\hat{N}_i, CW_{\min}, CW_{\max}, N_{\max}\}$
Result: $\{CW_i\}$
begin

1   **if** *($\hat{N}_i <= 1$)* **then**
2      $CW_i \leftarrow CW_{\min}$;
3   **else if** *($\hat{N}_i > 1$ && $\hat{N}_i <= N_{\max}$)* **then**
4      $CW_k \leftarrow CW_{\min}$;
5   *Compute p^** using (10) and (11);
6      $m \leftarrow p^*/CW_{\max}$;
7   **while** $\sigma > 1$ **do**
8        $CW_{k+1} \leftarrow CW_k - P(CW_k)/P'(CW_k)$;
9        $\sigma \leftarrow fabs(CW_{k+1} - CW_k)$;
10        $CW_k \leftarrow CW_{k+1}$;
11      $CW_i \leftarrow round(CW_{k+1})$;
12   **else if** *($\hat{N}_i > N_{\max}$)* **then**
13      $CW_i \leftarrow CW_{\max}$;
14   **return** CW_i;

---

used to compute the optimal size of the minimum contention window when $1 < \hat{N}_i \leq N_{\max}$ (see Line 3-11). Note that the optimal size of CW_i is computed with an accuracy (σ) of one slot (see Lines 7 and 9). Finally, the largest value of the minimum contention window $CW_{\max}$ is set in Lines 12-13.

D. POSACC ALGORITHM

POSACC controls the beacon transmission parameters based on the vehicle dynamics and surrounding situation. POSACC integrates the control mechanisms described above to provide the position accuracy and communication reliability required by cooperative safety applications. It also focuses on maintaining the vehicle's warning distance, channel load, and end-to-end latency into the operative range of cooperative safety applications.

POSACC takes advantage from the relationship between average velocity and traffic density [34] to reduce the conflict between the design goals. The interference is decreased

---

Algorithm 4 POSACC

Data: {data-set: Algorithm 1, Algorithm 2, Algorithm 3}
Result: $\{R_{b_i}, P_{T_i}, CW_i\}$
begin

1   Execute **Algorithm 1**;
2   Execute **Algorithm 2**;
3   Execute **Algorithm 3**;
4   **return** R_{b_i};
5   **return** P_{T_i};
6   **return** CW_i;

TABLE 2. Traffic settings.

Traffic Setup	1	2	3	4	5	6	7	8
Traffic Density (ρ) [veh/km/lane]	10	20	30	40	50	60	70	80
Maximum Velocity [km/h]	100	90	80	70	60	50	40	30

without affecting the position accuracy and warning distance. In addition, a balance between the end-to-end latency and beacon interval is maintained in order to avoid packet losses due to expiration time reached.

Algorithm 4 describes the steps followed by POSACC on each beacon transmission. First, the beacon rate is computed depending on vehicle movement status to guarantee the desired position accuracy (see Line 1). Then, the optimal vehicle's transmission power is computed to maximize the probability of successful reception at the target warning distance (see Line 2). Finally, the optimal size of the minimum contention window is computed depending on the maximum LDM database size reported in the neighborhood of the transmitting vehicle to minimize the probability of packet collisions (see Line 3).

IV. SIMULATION SETUP

This section presents the simulation setup in detail. The basic settings of the evaluation scenario, as well as communication parameters, are introduced in Section IV-A. The configurations of ETSI DMG, LIMERIC, DC-BTR&P and POSACC are given in Section IV-B.

A. SCENARIOS AND BASIC CONFIGURATION

We conduct our simulations using the Veins framework [43] with the IEEE 802.11p MAC/PHY model introduced by Eckhoff and Sommer in [44]. We assume a dedicated CCH that is solely used by safety applications. Consequently, the beaconing process occurs on the CCH without considering multi-channel operation. The evaluation scenario is a one-way two-lane highway with a total length of 3 km. Vehicles are randomly located on the first kilometer of the highway. To address a wide range of vehicular situations (e.g., from low vehicular density - high average speed to high vehicular density - low average speed), we define eight different traffic setups, as shown in Table 2.

The transmission power is set to 20 dBm [2]. We utilize the Two-Ray Interference model [45] with a dielectric constant $\epsilon_r = 1.02$ to simulate the radio signal propagation. This model has been validated based on an extensive set of road

TABLE 3. Simulation parameters.

Parameter	Value
CCH Frequency	5.89 GHz [2]
CCH Bandwidth	10 MHz [2]
Transmission Power	20 dBm [2]
Receiver Sensitivity	-82 dBm [19]
Carrier Sense Threshold	-90 dBm [19]
Thermal Noise	-104 dBm [25]
Data-Rate (R_D)	6 Mbps [4]
Beacon Size (b_z)	378 bytes [15]
Access Category (AC)	AC_VO [4], [13]
Backoff Slot Time	13 μs [4], [44]
Propagation Model	Two-Ray Interference [45]

measurements, capturing complex signal effects, especially at short and medium distances [45]. The beacons have 378 bytes [15] and are transmitted with a priority corresponding to the voice access category (AC_VO) [4], [13]. Each vehicle is 5 m long, 2 m wide, with a maximum acceleration of 2.5 m/s^2, and deceleration up to 4.5 m/s^2. We utilize omnidirectional antennas with a height of 1.5 m [38] and a data-rate equal to 6 Mbps [4]. In order to validate statistically the results, we conducted a total of 800 simulations with random seeds: 8 traffic setups, 5 beaconing algorithms configurations, and 20 repetitions. The most important simulation parameters are given in Table 3.

B. CONFIGURATION OF THE ALGORITHMS

POSACC is compared with two relevant state-of-the-art beaconing algorithms, such as ETSI DMG [7] and LIMERIC [15]. POSACC is also compared with our previous adaptive beaconing algorithm, DC-BTR&P [26]. We developed a new simulation model using the Veins framework, which captures the full operation mode of the four adaptive beaconing algorithms.

As specified in [7], ETSI DMG transmits a new CAM if one of the following conditions has been detected:

- The difference between current and previous position exceeds 4 m (e.g., $\Delta pos \geq 4$ m);
- The difference between current and previous velocity exceeds 0.5 m/s (e.g., $\Delta vel \geq 0.5$ m/s);
- The difference between current and previous heading exceeds 4° (e.g., $\Delta head \geq 4°$);

CAM trigger rules are checked at a time interval denoted as Status Monitoring and Decision Interval (SMDI).

In LIMERIC [15], each vehicle adapts its beacon transmission rate such that the channel load converges to a specified threshold. The beacon rate of vehicle j at time instant t is computed according to,

$$\hat{r}_j(t) = (1 - \alpha)\hat{r}_j(t - 1) + \beta(\hat{r}_g - \hat{r}_C(t - 1)), \quad (14)$$

where $\hat{r}_C$ is the aggregate rate of all vehicles participating in congestion control, $\hat{r}_g$ is the goal for the total rate, and α and β are adaptation parameters that control stability, fairness, and steady-state convergence.

To ensure convergence in very dense scenarios, LIMERIC introduces a novel gain saturation approach. The modified linear rate-control equation based on (14) with gain

saturation is,

$$\hat{r}_j(t) = (1 - \alpha)\hat{r}_j(t - 1)$$
$$+ \text{sign}(\hat{r}_g - \hat{r}_C(t - 1)) \min[X, \beta |(\hat{r}_g - \hat{r}_C(t - 1)|], \quad (15)$$

where X is a threshold that limits the update offset. We utilize LIMERIC with the gain saturation approach [15] for comparison purposes. The CBR is measured at a fixed time interval of 200 ms, as specified in [14]. This time interval is denoted as Channel Monitoring and Decision Interval (CMDI).

DC-BTR&P [26] adapts the beacon rate and transmission power of the vehicle j to provide the desired position accuracy. The beacon rate is adjusted according to the beacon rate control mechanism presented in Section III-A. The transmission power is computed as [26],

$$\hat{P}_{t_j} = \hat{P}_{t_{\min}} + (\hat{P}_{t_{\max}} - \hat{P}_{t_{\min}}) \left(1 - \frac{L_j}{L_o}\right) \hat{R}_{b_j}^{-\phi}, \quad (16)$$

where $\hat{P}_{t_{\min}}$ is a minimum fixed transmission power, $\hat{P}_{t_{\max}}$ is the maximum allowed transmission power, L_o is the channel load threshold, ϕ is a weight factor which controls the impact of the beacon rate $\hat{R}_{b_j}$ on the transmission power, and L_j is the channel load on j.

In POSACC, we specify an average position error of 1 m according to cooperative safety-critical applications, such as LCRW [10] and ICRW [11]. The critical beacon interval is set to 0.2 s [34], achieving a good trade-off between position tracking and the generated interference. We set a minimum warning distance of 50 m, which is within the minimum safety range used in [19]. We define a safety time of 5 s, that is long enough to include a maximum latency of 300 ms [10], [11], an average driver's reaction time of 1.5 s [36], a required action time of 0.75 s [37], and a margin of 2.45 s. To achieve a high probability of successful reception of beacon messages, the target reliability is set to 0.99. According to [4], an interval from 3 to 1023 is used for the contention window. As specified in [46], an optimal contention window must keep a balance between the expired beacons and the collided ones. Since the trade-off between communication reliability and end-to-end latency depends on $N_{\max}$, two different setups are investigated. We set the maximum value of $\hat{N}$ to 200 and 500 vehicles, which are values into the range of the vehicular density studied in [15]. The algorithms settings are shown in Table 4.

V. EVALUATION

POSACC relies on the adaptation of beacon rate, transmission power, and the size of the minimum contention window. Therefore, we first verify the aforementioned three points in Section V-A. Then, we present the performance of POSACC and compare it with ETSI DMG, LIMERIC, and DC-BTR&P in Section V-B.

A. PERFORMANCE OF THE CONTROL MECHANISMS

POSACC controls in real-time the beacon rate, transmission power, and the size of the minimum contention. Therefore,

TABLE 4. Algorithms settings.

| Algorithm	Parameter	Value
ETSI DMG	Δpos	$\geq$ 4 m [7]
ETSI DMG	Δvel	$\geq$ 0.5 m/s [7]
ETSI DMG	$\Delta head$	$\geq$ 4° [7]
ETSI DMG	SMDI	20 ms [7]
LIMERIC	alpha (α)	0.1 [15]
LIMERIC	beta (β)	1/150 [15]
LIMERIC	Goal for Total Rate ($\hat{r}_g$)	0.6 [15]
LIMERIC	Threshold (X)	0.0005 [15]
LIMERIC	CMDI	200 ms [14]
DC-BTR&P	Min. Transmission Power	7 dBm [26]
DC-BTR&P	Max. Transmission Power	20 dBm [26]
DC-BTR&P	Channel Load Threshold (L_o)	0.6 [15]
DC-BTR&P	Weight Factor (ϕ)	2 [26]
DC-BTR&P	Average Position Error ($\overline{E}$)	1 m [10], [11]
DC-BTR&P	Critical Beacon Interval (I_{b_c})	0.2 s [34]
POSACC	Average Position Error ($\overline{E}$)	1 m [10], [11]
POSACC	Critical Beacon Interval (I_{b_c})	0.2 s [34]
POSACC	Min. Warning Distance (d_{w_o})	50 m [19]
POSACC	Desired Safety Time (t_s)	5 s [37]
POSACC	Target Reliability (r_t)	0.99
POSACC	Maximum value of $\hat{N}$ ($N_{\max}$)	200, 500 [15]
POSACC	Minimum value of CW ($CW_{\min}$)	3 [4]
POSACC	Maximum value of CW ($CW_{\max}$)	1023 [4]
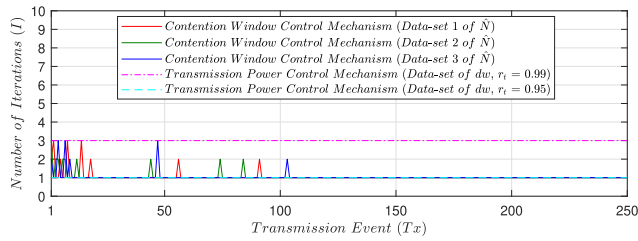
FIGURE 10. Complexity of the Newton-Raphson based control mechanism.

the first step is to evaluate the performance of the iteration processes. We use small scale Matlab simulations based on data-sets to evaluate the complexity of the iteration processes. Fig. 10 shows that the Newton-Raphson based control mechanisms solve the optimization problems with a really low number of iterations.

To better understand how POSACC reacts to vehicular traffic dynamics, we illustrate in Fig. 11 the acceleration and velocity of a generic vehicle in the scenario during 100 s of the simulation time. Since the impact of the acceleration on the beacon interval computed by the beacon rate control mechanism is more significant at lower velocities, we show the mobility pattern of the vehicle in the traffic scenario of 70 veh/km/lane (40 km/h).

Fig. 12a illustrates the adjustment that POSACC imposes in real-time on the beacon interval to achieve an average position error of 1 m. The beacon rate corresponding to the beacon interval required by POSACC is shown in Fig. 12b. In accelerated movement, an increase in velocity demands an increase in the beacon rate computed by POSACC, ensuring that for high-velocity situations the beacon interval is shortened to guarantee the target position accuracy, as shown in the interval from 10 s to 30 s. POSACC not only responds to variations in speed but also to changes of acceleration, as shown in the interval from 3 s to 10 s. In this time interval, the vehicle moves with a velocity of 6.2 m/s (22 km/h) and the beacon interval (beacon rate) oscillates between 0.32 s
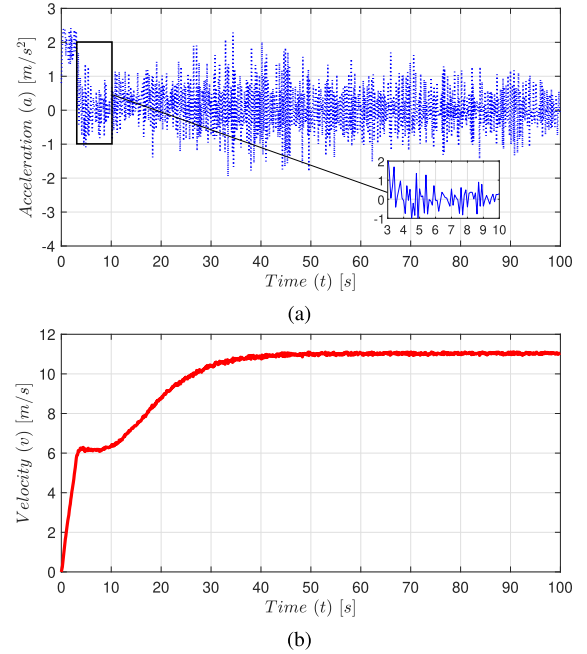
FIGURE 11. (a) Acceleration and (b) velocity developed by the vehicle during 100 s of simulation time with ρ = 70 veh/km/lane.
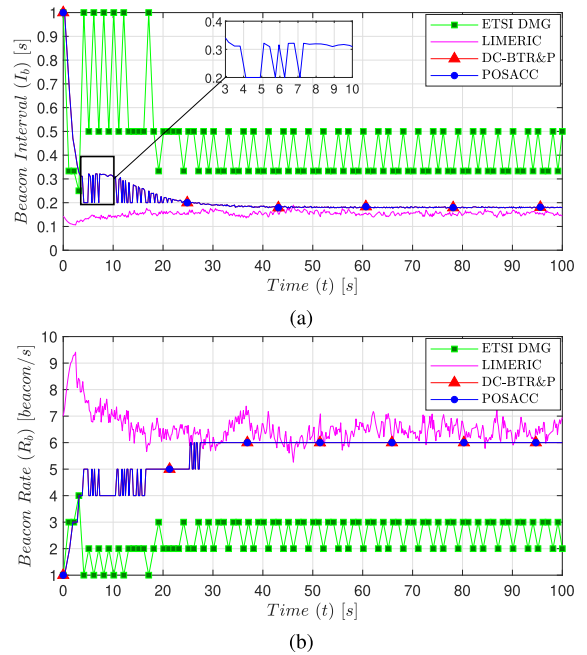
FIGURE 12. (a) Beacon interval and (b) beacon rate computed by the vehicle during 100 s of simulation time with ρ = 70 veh/km/lane.

(4 beacon/s) and 0.2 s (5 beacon/s). Positive or zero acceleration leads to a beacon interval close to 0.32 s, as predicted by (5) and (6) (see Fig. 4). Nevertheless, when the vehicle slows down, POSACC sets a critical beacon interval equal to 0.2 s. Consequently, surrounding vehicles are more likely to detect sudden braking.

For comparison purposes, we also include in Fig. 12 the beacon interval (beacon rate) computed by ETSI DMG and LIMERIC in the same traffic scenario. Note that POSACC
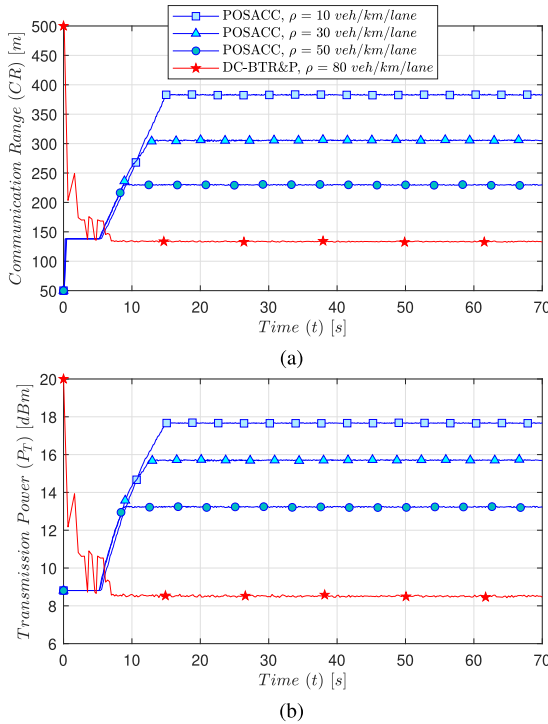
FIGURE 13. (a) Communication range and (b) transmission power computed by the vehicle for different traffic situations.

FIGURE 14. Size of the minimum contention window computed in real-time by the vehicles on different traffic situations with POSACC.

FIGURE 15. Transmission parameters computed by the beaconing algorithms.

and DC-BTR&P utilize the same beacon rate control mechanism. The vehicle dynamics is also taking into account by ETSI DMG. However, the asynchrony between the CAM trigger limit and the SMDI leads to oscillations in the beacon rate. For instance, if the vehicle has a constant speed of 12 m/s going straight ahead, it is expected that ETSI DMG generates exactly 3 beacon/s considering $\Delta pos \geq 4$ m (see [7]). Accordingly, the requirements of the vehicle dynamics are not fully fulfilled implying a potential risk for road safety. This divergence effect has been reported in [33]. On the contrary, POSACC achieves a stable beacon transmission rate once the velocity has increased and the impact of the acceleration is negligible, as shown in the interval from 30 s to 100 s. LIMERIC adjusts the beacon transmission rate based on the measured CBR without taking into account the specific vehicle dynamics. As specified in [30], noisy CBR measurements produce unfairness in rate allocation even with gain saturation.

Both POSACC and DC-BTR&P adapt the communication range and transmission power in real-time depending on vehicle dynamics, as shown in Fig. 13. Initially, the vehicle moves with low dynamics, so POSACC computes an intended communication range of 140 m to guarantee the default minimum warning distance of 50 m with reliability equal to 0.99. As velocity increases, POSACC increases the size of the safety shield by adjusting the warning distance to ensure a safety time of 5 s. For instance, in the traffic scenario of 30 veh/km/lane, the vehicle moves with a maximum velocity of 22.2 m/s (80 km/h) in the interval from
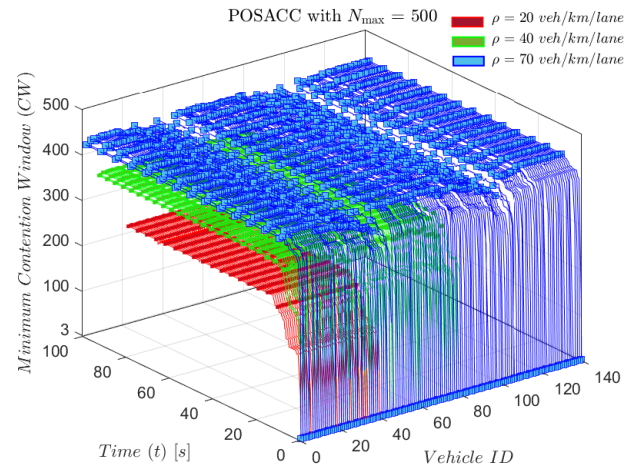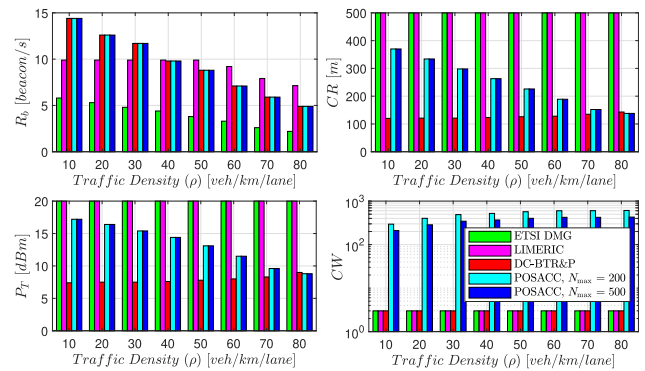
13 s to 70 s, resulting in a warning distance and intended communication range of 111 m and 310 m, respectively. Accordingly, POSACC increases the transmission power up to 15.7 dBm to maximize the probability of successful reception of beacon messages at the computed warning distance. In contrast, DC-BTR&P reduces the communication range and transmission power as the vehicle's velocity increases, as shown in Fig. 13. DC-BTR&P aims to mitigate packet collisions at the cost of decreasing the vehicle's warning distance. This strategy is suitable for urban environments where the vehicles' mobility pattern usually shows a continuous change between acceleration, deceleration, and repose (see [26]). However, on a highway, this issue is critical for road safety because drivers need to be notified at a sufficient distance from the expected impact, as specified in [10], [11]. Note that even in the traffic setup of the lowest velocity (80 veh/km/lane), the design of DC-BTR&P leads to a stable transmission power less than 9 dBm.

Fig. 14 demonstrates de effectiveness of POSACC to control the size of the minimum contention window in real-time on different traffic situations. Note that the dissemination of the maximum LDM database size ensures global fairness in the calculation of the optimal size of the mini-
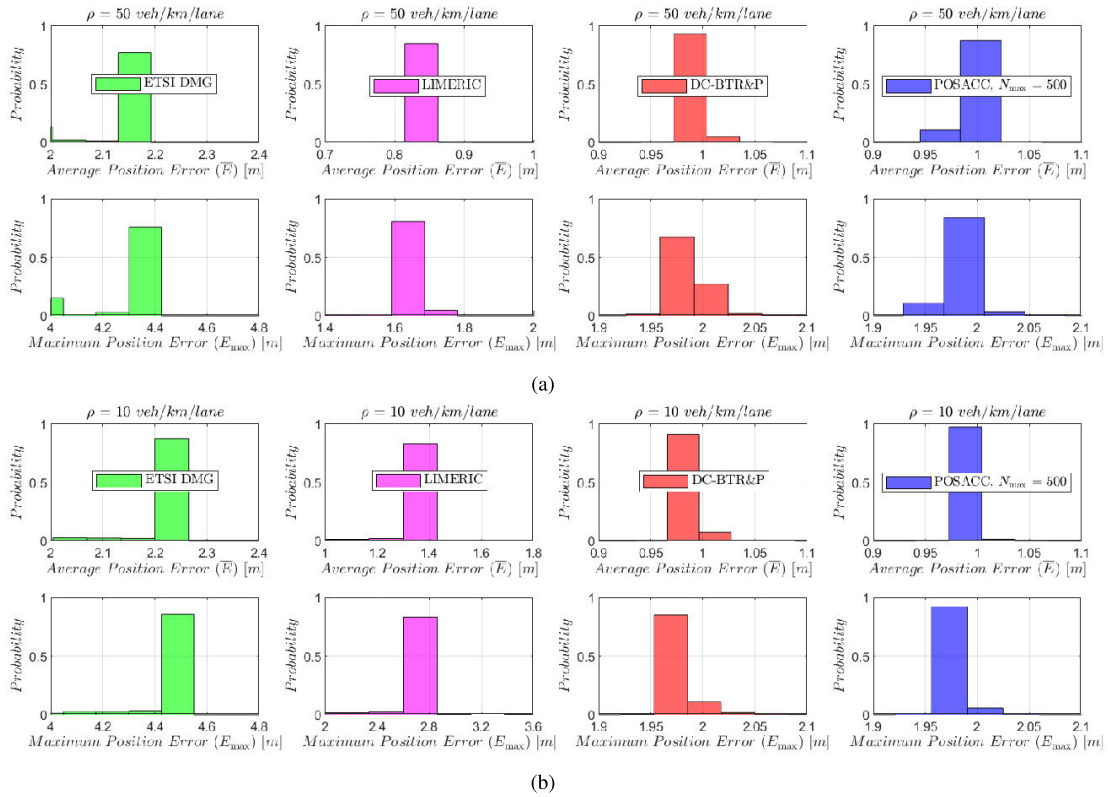
FIGURE 16. Probability-based histograms of the average and maximum position error achieved by the adaptive beaconing algorithms for (a) $\rho = 50$ veh/km/lane and (b) $\rho = 10$ veh/km/lane.

mum contention window, as well as the steady-state principle (see [40]). In POSACC, the size of the minimum contention window increases as more vehicles are registered in the LDM database, as defined by (12). Vehicles converge to the same optimal size of the minimum contention window. This not only minimizes the probability of packet collisions in the neighborhood of the transmitting vehicle but also decreases the negative impact of the hidden terminals.

Fig. 15 shows the average transmission parameters computed by the beaconing algorithms on each traffic scenario. POSACC adapts to vehicular traffic dynamics by using the proposed control mechanisms. Note that the design strategy reduces the conflict between the required goals. The beacon rate and transmission power decrease for higher traffic densities, since the velocity of the vehicles is reduced and more vehicles are involved in interferences. Further, the size of the minimum contention window decreases as the beacon rate increases because the traffic density is reduced and the end-to-end latency becomes more critical. For instance, in the traffic scenario of 10 veh/km/lane (100 km/h), POSACC increases the transmission rate up to 14 beacon/s to limit the average position error to 1 m, but at the same time, it sets the smallest size of the minimum contention window (e.g., 200 and 300) to reduce the latency and minimize the probability of packet collisions.

B. PERFORMANCE OF THE POSACC ALGORITHM

This subsection presents the evaluation results of POSACC compared with ETSI DMG, LIMERIC, and DC-BTR&P in terms of position accuracy, communication reliability, channel load, and end-to-end latency.

Fig. 16 shows the histograms with the relative probability of the average and maximum position error achieved by the beaconing algorithms in the traffic setups of 50 veh/km/lane (60 km/h) and 10 veh/km/lane (100 km/h). As defined by (1), the maximum position error is twice the average position error. We can observe the effectiveness of POSACC to achieve an average position error of 1 m. However, ETSI DMG only achieves half of the position accuracy provided by POSACC. Unlike ETSI DMG and POSACC, LIMERIC cannot guarantee a pre-defined position error. Note that the position error increases as the velocity of the vehicle increases. The reason is that LIMERIC controls the beacon transmission rate according to the channel load, without taking into account the vehicular traffic dynamics. The gain saturation technique limits the transmission rate to 10 beacon/s in low density - high speed scenarios (see Fig. 15). Despite that a beacon rate of 10 beacon/s provides a good position accuracy on a wide range of traffic conditions, this transmission rate is not enough to achieve an average position error of 1 m in vehicular scenarios where the velocity exceeds 80 km/h, as shown in Fig. 16b.
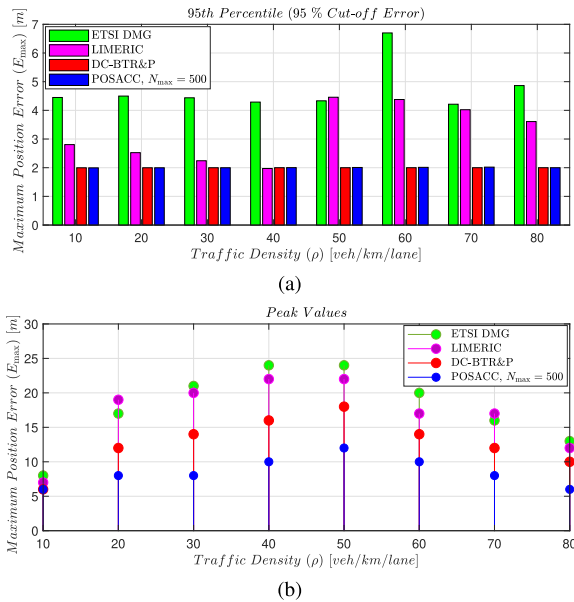
(a)

(b)

FIGURE 17. (a) 95 % cut-off and (b) peak values of the maximum position error achieved by the beaconing algorithms.

Fig. 17a illustrates that the position accuracy achieved by POSACC is better than the ETSI DMG and LIMERIC in each traffic setup. Note that 95 % of the maximum position error population falls below 2 m, which means that most of the vehicles compute an average position error of 1 m. Further, POSACC also achieves lower peaks of the maximum position error on all conditions, as shown in Fig. 17b. Both algorithms ETSI DMG and LIMERIC have limitations when applied to cooperative safety-critical applications. Trigger conditions in ETSI DMG lead to low beacon rates in order to alleviate the channel load and maintain a certain level of awareness. However, packet losses have more impact on position error at lower beacon rates. This means that for each beacon lost in ETSI DMG, the position error increases by 4 m. Accordingly, the peak values of the maximum position error in ETSI DMG increase up to 24 m, as shown in Fig. 17b. In addition, ETSI DMG has the worst performance in the traffic setup of 60 veh/km/lane, achieving a 95 % cut-off error higher than 6 m. This analysis is supported by the packet delivery ratio (PDR) shown in Fig. 18. The vertical lines in Fig. 18 represent the 25th and 75th percentiles. We can observe that the mean PDR achieved by ETSI DMG in the traffic setup of 60 veh/km/lane is below 0.92.

In LIMERIC, the gain saturation technique leads to a high beacon rate in low densities. Therefore, it only sets a beacon rate lower than 10 beacon/s if the traffic density is high, for example, when exceeds 50 veh/km/lane (see Fig. 15). If the beacon transmission rate is high, the impact of packet losses on the position error is lower. However, recurring packet losses eventually will lead to a higher position error, as shown in Fig. 17b. Note that the peaks of the maximum position error in LIMERIC are close to the peaks computed by ETSI DMG. This effect also can be observed in the traffic densities from
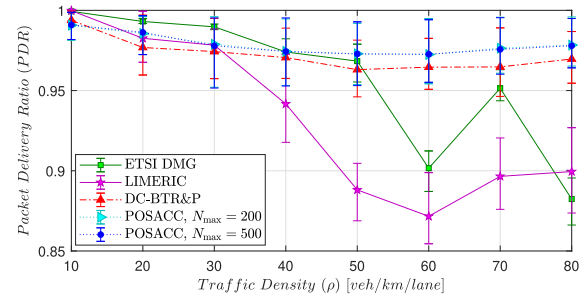

FIGURE 18. Packet delivery ratio computed by the beaconing algorithms on each traffic setup.

50 to 80 veh/km/lane, where the 95 % cut-off error achieved by LIMERIC increases up to 4 m (see Fig. 17a) and the mean PDR does not exceed 0.91 (see Fig. 18). For instance, it is expected that the maximum position error computed by LIMERIC be 1.4 m in the traffic density of 70 veh/km/lane (40 km/h). However, the 95 % cut-off maximum position error is almost three times higher than the expected value due to packet losses.

Fig. 18 shows that POSACC has also the best performance in terms of communication reliability, achieving a mean PDR higher than 0.95 for each traffic setup. The PDR achieved by LIMERIC decreases as traffic density increases. Since vehicles adjust the beacon rate to achieve fairness, it requires a great number of vehicles sharing the channel resources to set a low transmission rate. Fig. 15 shows that even in the more dense setups, the average beacon rate of LIMERIC is higher than 6 beacon/s. Consequently, more vehicles suffer from interference, leading to a higher packet collision rate, as shown in Fig. 19. This is critical in non-homogeneous scenarios where vehicles are moving at different speeds (e.g., a two-way highway in free flow and congested state). The interference generated by the congested section leads to a low position accuracy in the vehicles that move at high speed. ETSI DMG is also affected by vehicular density. We notice that controlling the beacon rate according to vehicle dynamics is not sufficient to guarantee a PDR higher than 0.95 on each traffic setup.

Fig. 20 shows that POSACC is able to regulate the channel load by adapting the beacon rate according to vehicle traffic dynamics. In this figure, the vertical lines also represent the 25th and 75th percentiles. As expected, ETSI DMG and LIMERIC measure the lower and higher CBR, respectively. ETSI DMG achieves a low CBR at the cost of reducing the position accuracy. Instead, LIMERIC maximizes channel utilization at the cost of reducing communication reliability. Whereas for POSACC, the measured CBR does not exceed 35 % of the channel capacity, and it is controlled by the relationship between the average velocity and traffic density (see [34]). Note that the CBR increases, then it remains stable and finally decreases. However, in the more dense traffic setups, the CBR measured by LIMERIC exceeds 50 % of channel capacity.
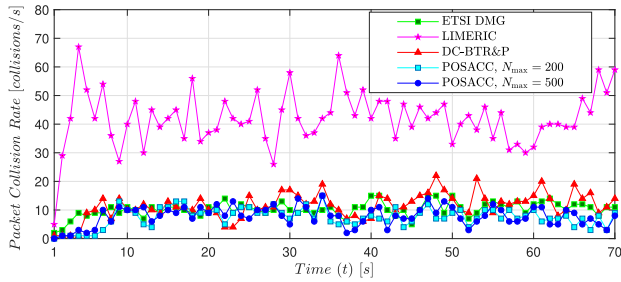
FIGURE 19. Packet collisions per second measured in the traffic setup of 60 veh/km/lane.
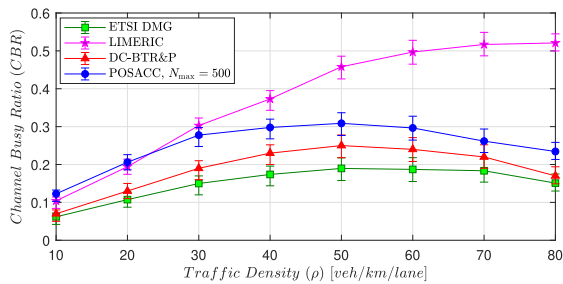

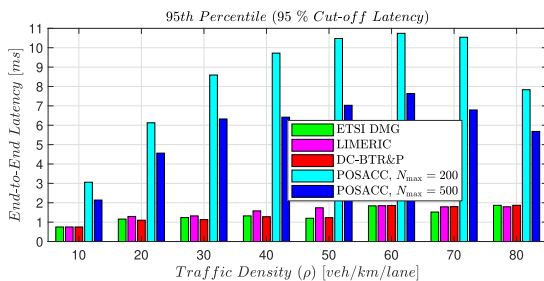**FIGURE 20.** Channel busy ratio computed by the beaconing algorithms on each traffic setup.

FIGURE 21. End-to-end latency performance (95 % cut-off latency) achieved by the beaconing algorithms.

In POSACC, the adaptive control of the minimum contention window provides a high position accuracy without significantly affecting communication reliability, as shown in Fig. 19. Note that POSACC and ETSI DMG compute a similar packet collision rate, but POSACC achieves a position accuracy two times higher. POSACC guarantees the priority metrics at the cost of increasing the end-to-end latency, as shown in Fig. 21. However, the 95 % cut-off end-to-end latency computed in all conditions are far away from the upper limit of 300 ms specified by ETSI for cooperative safety applications (see [10], [11]). In fact, the 95 % cut-off latency does not exceed 11 ms, and it is lower than 8 ms for $N_{max} = 500$. We notice that both setups of N_{max} achieve similar performance in terms of communication reliability (see Fig. 18); however, the setup of $N_{max} = 200$ leads to an increase in the latency up to 3 ms. POSACC keeps a balance between the end-to-end latency and beacon interval in order to avoid packet losses due to expiration time reached. Note that an increase in the end-to-end latency also corresponds to an increase in beacon interval (see Fig. 15). Accordingly,

POSACC provides the position accuracy and communication reliability required by cooperative safety applications with a 95 % cut-off latency that does not exceed 8 % of the beacon interval.

VI. CONCLUSION

In this paper, we proposed an adaptive beaconing algorithm, called POSACC, for cooperative vehicular safety systems. We designed three different control mechanisms to guarantee specific performance metrics. The performance of POSACC algorithm was evaluated in different traffic setups and compared against three different state-of-the-art beaconing algorithms; ETSI DMG, LIMERIC, and DC-BTR&P. Extensive evaluation results demonstrated that the design strategy was able to reduce the conflict between the required goals. The proposed control mechanisms proved their effectiveness to control the beacon transmission parameters in real-time. POSACC was able to limit the position error and improve communication reliability, while maintaining the warning distance, channel load, and end-to-end latency within the desired limits. POSACC outperformed the benchmark beaconing algorithms by guaranteeing the operational requirements of cooperative safety application in a wider range of traffic situations. POSACC achieved in each traffic setup a 95 % cut-off average position error of 1 m and PDR higher than 0.95, with a 95 % cut-off end-to-end latency that not exceeded 8 % of the beacon interval.

Regarding future work, we intend to study the benefits and limitations of controlling the values of CW_{max} and N_{max} in real-time according to the surrounding traffic situation, as well as using nonlinear functions in the contention window control mechanism.

REFERENCES

[1] E. Ahmed and H. Gharavi, "Cooperative vehicular networking: A survey," *IEEE Trans. Intell. Transp. Syst.*, vol. 19, no. 3, pp. 996–1014, Mar. 2018.

[2] *Wireless LAN Medium Access Control (MAC) and Physical Layer (PHY) Specifications; Amendment 6: Wireless Access in Vehicular Environments*, IEEE Standard 802.11p, 2010, pp. 1–35.

[3] *IEEE Guide for Wireless Access in Vehicular Environments (WAVE)— Architecture*, IEEE Standard 1609.0-2019 (Revision of IEEE Std 1609.0-2013), 2019, pp. 1–106.

[4] *IEEE Standard for Information Technology—Part 11: Wireless LAN Medium Access Control (MAC) and Physical Layer (PHY) Specifications*, IEEE Standard 802.11-2016 (Revision of IEEE Std 802.11-2012), 2016, pp. 1–3534.

[5] U. Hernandez-Jayo and I. De-la-Iglesia, "Reliability of cooperative vehicular applications on real scenarios over an IEEE 802.11 p communications architecture," in *Proc. Int. Conf. E-Bus. Telecommun. (ICETE)*, vol. 456. Berlin, Germany: Springer, 2014, pp. 387–401.

[6] *Dedicated Short Range Communications (DSRC) Message Set Dictionary*, SAE Standard J2735, 2016, pp. 1–267.

[7] *Intelligent Transport Systems (ITS); Vehicular Communications; Basic Set of Applications; Part 2: Specification of Cooperative Awareness Basic Service*, document ETSI EN 302 637-2 V1.4.1, 2019, pp. 1–45.

[8] G. Boquet, I. Pisa, J. L. Vicario, A. Morell, and J. Serrano, "Analysis of adaptive beaconing protocols for intersection assistance systems," in *Proc. 14th Annu. Conf. Wireless On-Demand Netw. Syst. Services (WONS)*, Isola, France, 2018, pp. 67–74.

[9] CAMP VSCC, "Vehicle safety communications project: Task 3 final report; identify intelligent vehicle safety applications enabled by DSRC," NHTSA, Washington, DC, USA, US DoT, Tech. Rep. DoT HS 809859, 2005, pp. 1–142.

[10] *Intelligent Transport Systems (ITS); V2X Applications; Part 3: Longitudinal Collision Risk Warning (LCRW) Application Requirements Specification*, document ETSI TS 101 539-3 V1.1.1, 2013, pp. 1–29.

[11] *Intelligent Transport Systems (ITS); V2X Applications; Part 2: Intersection Collision Risk Warning (ICRW) Application Requirements Specification*, document ETSI TS 101 539-2 V1.1.1, 2018, pp. 1–30.

[12] B. Shabir, M. A. Khan, A. U. Rahman, A. W. Malik, and A. Wahid, "Congestion avoidance in vehicular networks: A contemporary survey," *IEEE Access*, vol. 7, pp. 173196–173215, 2019.

[13] S. A. A. Shah, E. Ahmed, F. Xia, A. Karim, M. Shiraz, and R. M. Noor, "Adaptive beaconing approaches for vehicular ad hoc networks: A survey," *IEEE Syst. J.*, vol. 12, no. 2, pp. 1263–1277, Jun. 2018.

[14] T. Tielert, D. Jiang, Q. Chen, L. Delgrossi, and H. Hartenstein, "Design methodology and evaluation of rate adaptation based congestion control for vehicle safety communications," in *Proc. IEEE Veh. Netw. Conf. (VNC)*, Amsterdam, The Netherlands, Nov. 2011, pp. 116–123.

[15] G. Bansal, J. B. Kenney, and C. E. Rohrs, "LIMERIC: A linear adaptive message rate algorithm for DSRC congestion control," *IEEE Trans. Veh. Technol.*, vol. 62, no. 9, pp. 4182–4197, Nov. 2013.

[16] E. Egea-Lopez and P. Pavon-Marino, "Distributed and fair beaconing rate adaptation for congestion control in vehicular networks," *IEEE Trans. Mobile Comput.*, vol. 15, no. 12, pp. 3028–3041, Dec. 2016.

[17] *Intelligent Transport Systems (ITS); Decentralized Congestion Control Mechanisms for Intelligent Transport Systems Operating in the 5 GHz range; Access Layer Part*, document ETSI TS 102 687 V1.2.1, 2018, pp. 1–14.

[18] C.-L. Huang, Y. P. Fallah, R. Sengupta, and H. Krishnan, "Intervehicle transmission rate control for cooperative active safety system," *IEEE Trans. Intell. Transp. Syst.*, vol. 12, no. 3, pp. 645–658, Sep. 2011.

[19] M. Sepulcre, J. Gozalvez, O. Altintas, and H. Kremo, "Integration of congestion and awareness control in vehicular networks," *Ad Hoc Netw.*, vol. 37, pp. 29–43, Feb. 2016.

[20] F. Goudarzi and H. Asgari, "Non-cooperative beacon rate and awareness control for VANETs," *IEEE Access*, vol. 5, pp. 16858–16870, 2017.

[21] J. Aznar-Poveda, E. Egea-Lopez, A.-J. Garcia-Sanchez, and P. Pavon-Marino, "Time-to-collision-based awareness and congestion control for vehicular communications," *IEEE Access*, vol. 7, pp. 154192–154208, 2019.

[22] N. Haouari, S. Moussaoui, and S. Senouci, "Application reliability analysis of density-aware congestion control in VANETs," in *Proc. IEEE Int. Conf. Commun. (ICC)*, Kansas City, MO, USA, May 2018, pp. 1–6.

[23] J. Breu, A. Brakemeier, and M. Menth, "A quantitative study of cooperative awareness messages in production VANETs," *EURASIP J. Wireless Commun. Netw.*, vol. 98, pp. 1–18, Dec. 2014.

[24] M. Torrent-Moreno, M. Killat, and H. Hartenstein, "The challenges of robust inter-vehicle communications," in *Proc. IEEE 62nd Veh. Technol. Conf. (VTC-Fall)*, Dallas, TX, USA, Jan. 2005, pp. 319–323.

[25] R. K. Schmidt, T. Köllmer, T. Leinmüller, B. Böddeker, and G. Schäfer, "Degradation of transmission range in VANETs caused by interference," *PIK-Praxis der Informationsverarbeitung Kommunikation*, vol. 32, no. 4, pp. 224–234, 2009.

[26] S. Bolufé, S. Montejo-Sánchez, C. A. Azurdia-Meza, S. Céspedes, R. D. Souza, and E. M. G. Fernandez, "Dynamic control of beacon transmission rate and power with position error constraint in cooperative vehicular networks," in *Proc. 33rd Annu. ACM Symp. Appl. Comput. (SAC)*, Pau, France, 2018, pp. 2084–2091.

[27] *Intelligent Transport Systems (ITS); ITS-G5 Access Layer Specification for Intelligent Transport Systems Operating in the 5 GHz Frequency Band*, document ETSI EN 302 663 V1.3.0, 2019, pp. 1–24.

[28] *Intelligent Transport Systems (ITS); Cross Layer DCC Management Entity for Operation in the ITS G5A and ITS G5B medium; Validation Set-Up and Results*, document ETSI TR 101 613 V1.1.1, 2015, pp. 1–50.

[29] *Intelligent Transport Systems (ITS); Vehicular Communications; Basic Set of Applications; Part 3: Specifications of Decentralized Environmental Notification Basic Service*, document ETSI EN 302 637-3 V1.3.1, 2019, pp. 1–74.

[30] B. Kim, I. Kang, and H. Kim, "Resolving the unfairness of distributed rate control in the IEEE WAVE safety messaging," *IEEE Trans. Veh. Technol.*, vol. 63, no. 5, pp. 2284–2297, Jun. 2014.

[31] Y. Yao, X. Chen, L. Rao, X. Liu, and X. Zhou, "LORA: Loss differentiation rate adaptation scheme for vehicle-to-vehicle safety communications," *IEEE Trans. Veh. Technol.*, vol. 66, no. 3, pp. 2499–2512, Mar. 2017.

[32] N. Lyamin, A. Vinel, M. Jonsson, and B. Bellalta, "Cooperative awareness in VANETs: On ETSI EN 302 637-2 performance," *IEEE Trans. Veh. Technol.*, vol. 67, no. 1, pp. 17–28, Jan. 2018.

[33] T. Lorenzen and H. Tchouankem, "Evaluation of an awareness control algorithm for VANETs based on ETSI EN 302 637-2 V1.3.2," in *Proc. IEEE Int. Conf. Commun. Workshop (ICCW)*, London, U.K., Jun. 2015, pp. 2458–2464.

[34] R. Schmidt, T. Leinmuller, E. Schoch, F. Kargl, and G. Schafer, "Exploration of adaptive beaconing for efficient intervehicle safety communication," *IEEE Netw.*, vol. 24, no. 1, pp. 14–19, Jan. 2010.

[35] M. van Eenennaam, W. K. Wolterink, G. Karagiannis, and G. Heijenk, "Exploring the solution space of beaconing in VANETs," in *Proc. IEEE Veh. Netw. Conf. (VNC)*, Tokyo, Japan, Oct. 2009, pp. 1–8.

[36] C. Chen, X. Liu, H.-H. Chen, M. Li, and L. Zhao, "A rear-end collision risk evaluation and control scheme using a Bayesian network model," *IEEE Trans. Intell. Transp. Syst.*, vol. 20, no. 1, pp. 264–284, Jan. 2019.

[37] Y. Chen, K. Shen, and S. Wang, "Forward collision warning system considering both time-to-collision and safety braking distance," in *Proc. IEEE 8th Conf. Ind. Electron. Appl. (ICIEA)*, Melbourne, VIC, Australia, Jun. 2013, pp. 972–977.

[38] M. Killat, F. Schmidt-Eisenlohr, H. Hartenstein, C. Rössel, P. Vortisch, S. Assenmacher, and F. Busch, "Enabling efficient and accurate large-scale simulations of VANETs for vehicular traffic management," in *Proc. 4th ACM Int. Workshop Veh. Ad Hoc Netw. (VANET)*, Montreal, QC, Canada, 2007, pp. 29–38.

[39] O. Chakroun and S. Cherkaoui, "Enhancing safety messages dissemination over 802.11p/DSRC," in *Proc. 38th Annu. IEEE Conf. Local Comput. Netw.-Workshops*, Sydney, NSW, Australia, Oct. 2013, pp. 179–187.

[40] G. Bianchi, "Performance analysis of the IEEE 802.11 distributed coordination function," *IEEE J. Sel. Areas Commun.*, vol. 18, no. 3, pp. 535–547, Mar. 2000.

[41] M. A. Karabulut, A. F. M. S. Shah, and H. Ilhan, "Performance modeling and analysis of the IEEE 802.11 DCF for VANETs," in *Proc. 9th Int. Congr. Ultra Modern Telecommun. Control Syst. Workshops (ICUMT)*, Munich, Germany, Nov. 2017, pp. 346–351.

[42] X. Lei and S. H. Rhee, "Performance analysis and enhancement of IEEE 802.11p beaconing," *EURASIP J. Wireless Commun. Netw.*, vol. 61, pp. 1–10, Dec. 2019.

[43] *Vehicles in Network Simulation (VEINS)*. Accessed: Jun. 7, 2019. [Online]. Available: https://veins.car2x.org/

[44] D. Eckhoff and C. Sommer, "A multi-channel IEEE 1609.4 and 802.11p EDCA model for the veins framework," in *Proc. 5th ACM/ICST Int. Conf. Simulation Tools Techn. Commun., Netw. Syst. (SIMUTools)*, Desenzano del Garda, Italy, 2012, pp. 1–2.

[45] C. Sommer, S. Joerer, and F. Dressler, "On the applicability of two-ray path loss models for vehicular network simulation," in *Proc. IEEE Veh. Netw. Conf. (VNC)*, Seoul, South Korea, Nov. 2012, pp. 64–69.

[46] R. Stanica, E. Chaput, and A. Beylot, "Local density estimation for contention window adaptation in vehicular networks," in *Proc. IEEE 22nd Int. Symp. Pers., Indoor Mobile Radio Commun.*, Toronto, ON, Canada, Sep. 2011, pp. 730–734.

SANDY BOLUFÉ received the B.Sc. degree in electronics and telecommunications engineering and the M.Sc. degree in telematics from the Central University of Las Villas (UCLV), Cuba, in 2009 and 2016, respectively. He is currently pursuing the Ph.D. degree with the Department of Electrical Engineering, Universidad de Chile, Santiago, Chile. From September 2009 to April 2017, he worked as a Professor with the Department of Telecommunications, UCLV. He is a member of the Enabling REsilient urban TRAnsportation systems in smart CiTies (ERANeT LAC) Project and the Wireless Networking Research Group (WiNet), the University of Chile. His research interests include cooperative communications and networking for automated and semi-automated vehicles, context-aware distributed algorithms, dissemination and routing protocols, and vehicular architectures.

CESAR A. AZURDIA-MEZA (Member, IEEE) received the B.Sc. degree in electrical engineering from the Universidad del Valle de Guatemala, Guatemala, in 2005, the M.Sc. degree in electrical engineering from Linnaeus University, Sweden, in 2009, and the Ph.D. degree in electronics and radio engineering from Kyung Hee University, South Korea, in 2013. He joined the Department of Electrical Engineering, University of Chile, as an Assistant Professor in August 2013, where he is currently lecturing on wireless and mobile communication systems. His research interests include topics such as Nyquist's ISI criterion, OFDM-based systems, SC-FDMA, visible light communication systems, vehicular communications, 5G and beyond enabling technologies, and signal processing techniques for communication systems. He is an IEEE Communications Society Member and a member of the IEICE Communications Society. He has served as a Technical Program Committee (TPC) Member for multiple conferences, and a Reviewer in journals such as the IEEE Communications Letters, the IEEE Transactions on Wireless Communications, *Wireless Personal Communications*, IEEE Access, *IET Communications*, *EURASIP Journal on Advances in Signal Processing*, among others. He was a co-recipient of the 2019 IEEE LATINCOM Best Paper Award and the 2016 IEEE CONESCAPAN Best Paper Award.

SANDRA CÉSPEDES (Senior Member, IEEE) received the B.Sc. and Specialization (2007) degrees in telematics engineering, and management of information systems from Universidad Icesi, Cali, Colombia, in 2003 and 2007, respectively, and the Ph.D. degree in electrical and computer engineering from the University of Waterloo, Canada, in 2012. She is currently an Assistant Professor with the Department of Electrical Engineering, Universidad de Chile, Santiago, Chile. She also holds an Honorary Adjunct Professor with Universidad Icesi. She is also the Head of research with NIC Chile Research Labs. Her research focuses on the topics of vehicular communications systems and networking, cyber-physical systems, smart grid communications, and routing and protocols design for the Internet of Things. She serves as an Associate Editor for the IEEE Internet of Things Journal.

SAMUEL MONTEJO-SÁNCHEZ (Member, IEEE) was born in Camagüey, Cuba, in 1979. He received the B.Sc., M.Sc., and D.Sc. degrees in telecommunications from the Central University of Las Villas (UCLV), Cuba, in 2003, 2007 and 2013, respectively. From September 2003 to May 2017, he was an Associate Professor with the Department of Telecommunications, UCLV. From February to July 2011, he was a Visiting Ph.D. Student with the Federal University of Technology (UTFPR), Brazil. In 2017, he has held a postdoctoral position with the University of Chile. Since 2018, he has been with the Programa Institucional de Fomento a la I+D+i (PIDi), Universidad Tecnológica Metropolitana (UTEM). He is a member of the FONDECYT Postdoctoral Grant 3170021 (Asignación de Recursos de Transmisión con Equidad en Comunicaciones Inalámbricas Energéticamente Eficientes), ERANeT LAC (Enabling REsilient urban TRAnsportation systems in smart CiTies), STIC AnSud (VLmC—Visible Light Mine Communications), FONDEF IT17M10012 (Multiuser VLC for underground mining), and FONDEQUIP EQM180180 (Clúster Supermicro para Cómputo Científico) projects. His research interests are in the areas of wireless communications, cognitive radio, network coding, energy efficiency, vehicular ad hoc networks, physical layer security, and the Internet of Things. He was a co-recipient of the 2016 Research Award from the Cuban Academy of Sciences.

RICHARD DEMO SOUZA (Senior Member, IEEE) was born in Florianópolis, Brazil. He received the B.Sc. and D.Sc. degrees in electrical engineering from the Federal University of Santa Catarina (UFSC), Brazil, in 1999 and 2003, respectively. In 2003, he was a Visiting Researcher with the Department of Electrical and Computer Engineering, University of Delaware, USA. From 2004 to 2016, he was with the Federal University of Technology—Paraná (UTFPR), Brazil. Since 2017, he has been with the Federal University of Santa Catarina (UFSC), Brazil, where he is currently an Associate Professor. His research interests are in the areas of wireless communications and signal processing. He is a Senior Member of the Brazilian Telecommunications Society (SBrT). He was a co-recipient of the 2014 IEEE/IFIP Wireless Days Conference Best Paper Award, the Supervisor of the awarded Best Ph.D. Thesis in Electrical Engineering in Brazil in 2014, and a co-recipient of the 2016 Research Award from the Cuban Academy of Sciences. He has served as an Editor-in-Chief of the *SBrT Journal of Communication and Information Systems* and an Associate Editor for the IEEE Communications Letters, the *EURASIP Journal on Wireless Communications and Networking*, and the IEEE Transactions on Vehicular Technology.

EVELIO M. G. FERNÁNDEZ (Member, IEEE) was born in Santa Clara, Cuba, in 1962. He received the B.Sc. degree from the Central University of Las Villas, Santa Clara, Cuba, in 1985, and the M.Sc. and D.Sc. degrees from the State University of Campinas, Brazil, in 1997 and 2001, respectively, all in electrical engineering. He is currently an Associate Professor with the Department of Electrical Engineering, Federal University of Paraná, Brazil. His research interests include channel coding techniques, digital communications, wireless networks, and cognitive radio systems. He is currently a member of the Brazilian Telecommunications Society. He was a co-recipient of the 2016 Research Award from the Cuban Academy of Sciences.

• • •